The myotubularin phosphatase MTMR4 regulates sorting from early endosomes

Monica J. Naughtin[1],*, David A. Sheffield[1],*, Parvin Rahman[1], William E. Hughes[2], Rajendra Gurung[1], Jennifer L. Stow[3], Harshal H. Nandurkar[4], Jennifer M. Dyson[1] and Christina A. Mitchell[1],‡

[1]Department of Biochemistry and Molecular Biology, Monash University, Wellington Road Clayton, 3800, Australia
[2]Diabetes and Obesity Research Program, Garvan Institute of Medical Research, 384 Victoria Street, Sydney, New South Wales, 2010, Australia
[3]Institute for Molecular Bioscience, University of Queensland, Brisbane, Queensland, 4072, Australia
[4]Department of Medicine, University of Melbourne, St. Vincent's Hospital, 41 Victoria Parade, Fitzroy, Victoria, 3065, Australia
*These authors contributed equally to this work
‡Author for correspondence (christina.mitchell@med.monash.edu.au)

Summary

Phosphatidylinositol 3-phosphate [PtdIns(3)P] regulates endocytic trafficking and the sorting of receptors through early endosomes, including the rapid recycling of transferrin (Tfn). However, the phosphoinositide phosphatase that selectively opposes this function is unknown. The myotubularins are a family of eight catalytically active and six inactive enzymes that hydrolyse PtdIns(3)P to form PtdIns. However, the role each myotubularin family member plays in regulating endosomal PtdIns(3)P and thereby endocytic trafficking is not well established. Here, we identify the myotubularin family member MTMR4, which localizes to early endosomes and also to Rab11- and Sec15-positive recycling endosomes. In cells with MTMR4 knockdown, or following expression of the catalytically inactive MTMR4, MTMR4^{C407A}, the number of PtdIns(3)P-decorated endosomes significantly increased. MTMR4 overexpression delayed the exit of Tfn from early endosomes and its recycling to the plasma membrane. By contrast, expression of MTMR4^{C407A}, which acts as a dominant-negative construct, significantly accelerated Tfn recycling. However, in MTMR4 knockdown cells Tfn recycling was unchanged, suggesting that other MTMs might also contribute to recycling. MTMR4 regulated the subcellular distribution of Rab11 and, in cells with RNAi-mediated knockdown of MTMR4, Rab11 was directed away from the pericentriolar recycling compartment. The subcellular distribution of VAMP3, a v-SNARE protein that resides in recycling endosomes and endosome-derived transport vesicles, was also regulated by MTMR4. Therefore, MTMR4 localizes at the interface of early and recycling endosomes to regulate trafficking through this pathway.

Key words: MTMR4, Myotubularin, Recycling endosomes, Tfn, FYVE domain

Introduction

The endocytic pathway comprises a complex network of discrete compartments and regulates the flow and destination of internalized cargo. All internalized molecules are transported to early endosomes, which sort cargo to specific destinations. Here, signalling receptors, such as the epidermal growth factor (EGF) receptor, separate from their ligands and the receptors are delivered to late endosomes and lysosomes for degradation (Gruenberg, 2001). Nutrient receptors that bind cargo such as transferrin (Tfn) enter early endosomes and recycle to the plasma membrane directly via a fast pathway, or return to the plasma membrane via the slow endocytic recycling compartment (Hopkins et al., 1994; Sheff et al., 1999; Hao and Maxfield, 2000; Sheff et al., 2002).

Phosphatidylinositol 3-phosphate [PtdIns(3)P)] is constitutively synthesized on early endosomes by the class III phosphoinositide 3-kinase (PI3K) complex, hVps34/hVps15 (Christoforidis et al., 1999; Johnson et al., 2006). PtdIns(3)P binds Hrs and Sara via their FYVE domains (Gaullier et al., 1998; Panopoulou et al., 2002) and also facilitates the endosomal recruitment of Rab5-effectors, EEA1 and Rabenosyn-5 (Nielsen et al., 2000). PtdIns(3)P regulates early endosomal fusion (Gorvel et al., 1991; McBride et al., 1999), the rate of endosome motility along microtubules (Nielsen et al., 1999), Tfn receptor (Tfn-R) recycling (van Dam et al., 2002), the sorting and degradation of internalized growth factor receptors (Petiot et al., 2003; Johnson et al., 2006), and retrograde trafficking from endosomes to the Golgi (Cozier et al., 2002; Carlton et al., 2004; Rojas et al., 2007). PtdIns(3)P is also a substrate for the PIKfyve kinase, generating phosphatidylinositol 3,5-bisphosphate [PtdIns(3,5)P_2] (Ikonomov et al., 2001) on early or late endosomes. PtdIns(3,5)P_2 regulates vacuolar membrane homeostasis, lysosomal homeostasis and the sorting of biosynthetic cargo and proteins into the vacuolar/lysosomal lumen (Gary et al., 1998; Odorizzi et al., 1998; Dove et al., 2002; Ikonomov et al., 2002; Rutherford et al., 2006).

The cellular levels of PtdIns(3)P and PtdIns(3,5)P_2 are tightly regulated by both the lipid kinases that synthesize these phosphoinositides and the phosphatases that hydrolyse these signals (Robinson and Dixon, 2006). In vitro, PtdIns(3)P and PtdIns(3,5)P_2 are hydrolysed at the 3-position phosphate by the myotubularin (MTM) family of lipid 3-phosphatases to form PtdIns and PtdIns(5)P, respectively (Blondeau et al., 2000; Walker et al., 2001; Berger et al., 2002; Begley et al., 2003; Schaletzky et al., 2003). Eight active myotubularin phosphatases have been identified, all of which contain a catalytic CX$_5$R motif. In addition, six catalytically inactive myotubularins have been described that contain mutations in the CX$_5$R motif (Robinson and Dixon, 2006). Heteromeric interactions between active and non-active myotubularins enhances the lipid 3-phosphatase activity and/or subcellular localization of the catalytically active phosphatases (Kim et al., 2003; Mochizuki and Majerus, 2003; Nandurkar et al.,

2003; Robinson and Dixon, 2005; Berger et al., 2006). The gene expressing founding family member myotubularin (MTM1) is the candidate gene mutated in X-linked myotubular myopathy, a syndrome associated with muscle weakness, hypotonia and early death (Laporte et al., 1996). Mutations in both active and inactive myotubularin phosphatases lead to human disease. Myotubularin myopathy-related protein 2 (MTMR2) mutation is associated with Charcot-Marie-Tooth disease type 4B1, and mutation in the inactive MTMR13 leads to a similar clinical syndrome (Bolino et al., 2000; Berger et al., 2002; Azzedine et al., 2003; Senderek et al., 2003).

The relationship between the subcellular localization and function of myotubularin phosphatases is poorly understood (Tsujita et al., 2004; Lorenzo et al., 2006). PtdIns(3)P localizes to early endosomes and multivesicular bodies (Gillooly et al., 2000; Gillooly et al., 2003). PtdIns(3,5)P_2 is implicated in late endosomal/lysosomal function, although early endosomal effects have also been described (Dove et al., 2009). The evidence for the subcellular distribution of MTMs to early or late endosomal compartments is conflicting, in part due to a general problem in generating specific immunoreactive MTM antibodies (Robinson and Dixon, 2006), so that most reports have relied on recombinant MTM overexpression to evaluate enzyme subcellular localization. Initial studies showed recombinant MTM1 localized to the cytosol (Kim et al., 2002; Laporte et al., 2002; Nandurkar et al., 2003; Schaletzky et al., 2003); however, more recent reports suggest that MTM1 localizes to early and/or late endosomes and regulates EGF receptor degradation (Cao et al., 2007; Cao et al., 2008). MTM1 siRNA (short interfering RNA) knockdown blocks EGFR degradation, inhibiting the receptor trafficking from endosomes to the lysosome. MTMR2 localizes to late endosomes and also contributes to signalling EGF receptor trafficking and degradation. Recently, a little-characterized MTM, MTMR4, was localized to early endosomes on the basis of recombinant overexpression; however, MTMR4 function is unknown (Lorenzo et al., 2006). Interestingly, a recent report has shown that MTMR4 interacts with and regulates phosphorylated R-Smads in early endosomes (Yu et al., 2010). MTMR4 contains an N-terminal PH-GRAM domain, a central myotubularin homology region (MTMHR) and a coiled-coil motif followed by a C-terminal FYVE domain (Zhao et al., 2001; Robinson and Dixon, 2006). In MTMR3, the PH domain binds PtdIns(5)P and perhaps PtdIns(3,5)P_2, and MTMR3 localizes to the cytosol and, under some conditions, to the endoplasmic reticulum and/or the Golgi (Walker et al., 2001; Lorenzo et al., 2005).

The subcellular sites at which MTMs hydrolyse PtdIns(3)P and/or PtdIns(3,5)P_2 are of significant interest because this could govern PtdIns(3)P-dependent trafficking. Here, we demonstrate that MTMR4 localizes at the interface between early and recycling endosomes and regulates the sorting of endosomal cargo such as Tfn into recycling endosomes. These studies identify MTMR4 as a novel regulator of endosomal trafficking.

Results

MTMR4 localizes to early and recycling endosomes

To examine the intracellular localization of MTMR4, antibodies were generated against the MTMR4 peptide sequence (amino acids 1092–1107) located within the FYVE domain (Fig. 1A). Affinity-purified antibodies were used to probe COS1 cells by immunoblot analysis and indirect immunofluorescence. MTMR4 anti-peptide antibodies immunoblotted a single immunoreactive species in COS1 cell lysates that migrated at ~170 kDa (see supplementary material Fig. S1A, left panel), higher than its
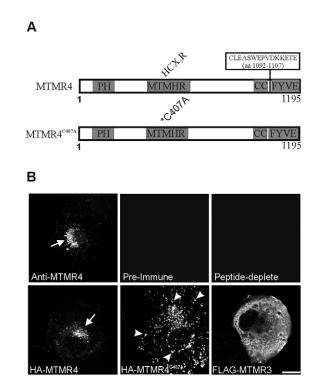

Fig. 1. Endogenous and recombinant MTMR4 localizes to endosomes. (**A**) MTMR4 constructs showing PH domain (PH), a central myotubularin homology region (MTMHR) containing the HCX$_5$R catalytic motif, coiled-coil (CC) and FYVE domains. The peptide sequence (amino acids 1092–1107) used as an immunogen is shown (boxed). The MTMR4^{C407A} construct contains a mutation of the catalytic cysteine to alanine at amino acid 407. (**B**) Upper panels: COS1 cells were immunostained with MTMR4 antibodies (Anti-MTMR4), pre-immune serum (Pre-Immune), or peptide preabsorbed MTMR4-immune serum (Peptide-deplete), and visualized by confocal microscopy. Lower panels: COS1 cells expressing HA–MTMR4, HA–MTMR4^{C407A} or FLAG–MTMR3 were stained with HA or FLAG antibodies and visualized by confocal microscopy. Arrow indicates perinuclear MTMR4 localization. Arrowheads show dispersed vesicular localization of HA–MTMR4^{C407A}. Scale bar: 20 μm.

predicted molecular mass of 130 kDa, which decreased to 130 kDa following treatment of cell lysates with alkaline phosphatase (not shown). Recombinant haemagglutinin (HA)-tagged MTMR4 also migrated at 170 kDa, as detected by HA immunoblot analysis (supplementary material Fig. S1A, right panel), suggesting phosphorylation or other post-translational modifications. The MTMR4 antibody also detected HA–MTMR4 and the isolated MTMR4 CC+FYVE domain (amino acids 1022–1175) to which the antibody was raised (not shown).

The MTMR4 antibody labelled punctate vesicles, which were reminiscent of endocytic organelles, with prominent staining in a perinuclear distribution (Fig. 1B, upper left panel, see arrow); however, faint cytosolic staining was also noted and, like other myotubularin antibodies, this antibody was not of high affinity (not shown). MTMR4 antibody staining was reduced in cells in which MTMR4 protein expression was reduced by siRNA (supplementary material Fig. S1B). Pre-immune and peptide-depleted serum was non-reactive (Fig. 1B, upper middle and right panel). COS1 cells were transiently transfected with MTMR3 or MTMR4. In agreement with previous reports, FLAG–MTMR3 exhibited diffuse cytosolic staining (Zhao et al., 2001; Lorenzo et
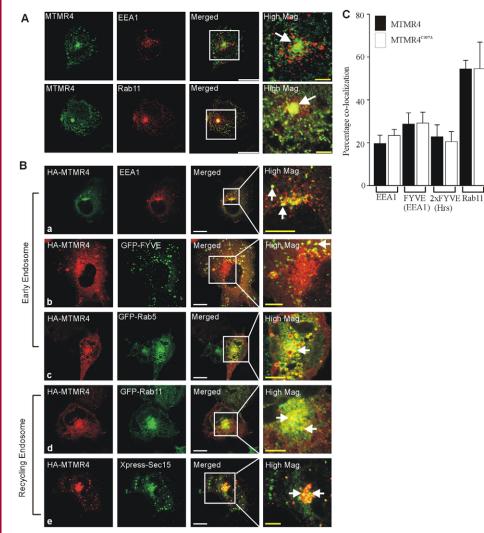
Fig. 2. MTMR4 localizes to early and recycling endosomes. (**A**) COS1 cells were immunostained with MTMR4 and EEA1 (upper panel), or Rab11 (lower panel) antibodies, and visualized by confocal microscopy. High magnification images are shown on far right. Arrows indicate colocalization. White scale bars: 20 µm, yellow scale bars: 10 µm. (**B**) COS1 cells transiently transfected with HA–MTMR4 (a), or co-transfected with GFP–FYVE (b), GFP–Rab5 (c), GFP–Rab11 (d), or Xpress–Sec15 (e). Cells were fixed, permeabilized and co-immunostained with HA and EEA1 (a), HA (b–d), or HA and Xpress antibodies (e), and visualized by confocal microscopy. The far right panel displays high magnification merged images corresponding to the boxed region. Arrows indicate colocalization. White scale bars: 20 µm, yellow scale bars: 10 µm. (**C**) Quantification of colocalization was conducted using AnalySIS software, with the pixel threshold adjusted to ten times the background. Results represent the mean percentage colocalization of MTMR4 (black bars) or MTMR4^{C407A} (white bars) with the indicated marker protein ± s.e.m. of 10 cells scored per marker protein.

al., 2006) (Fig. 1B, lower right panel), whereas HA–MTMR4 localized to punctate vesicles (Fig. 1B, lower left panel, see arrow).

Wild-type MTMR4 hydrolysed PtdIns(3)P, as reported (Zhao et al., 2001) and, although not previously shown, also hydrolysed PtdIns(3,5)P_2 (supplementary material Fig. S1C). We next generated a catalytically inactive HA–MTMR4^{C407A} mutant by introduction of a cysteine to alanine mutation in the CX$_5$R catalytic site (C407A) (Fig. 1A), resulting in complete loss of MTMR4 phosphatase activity (see supplementary material Fig. S1C, lower panels). This mutation in MTM1, MTMR2 and MTMR3 functions as a dominant-negative (Blondeau et al., 2000; Taylor et al., 2000; Walker et al., 2001; Berger et al., 2002). HA–MTMR4^{C407A} decorated cytosolic endocytic vesicles and showed less perinuclear distribution than wild-type MTMR4 (Fig. 1B, lower middle panel).

We next performed colocalization of endogenous MTMR4 with endosomal markers. Endogenous MTMR4-decorated vesicles showed significant, but only partial, colocalization with early endosomal antigen (EEA1) (Fig. 2A, top panel). Rab11 is a small guanine triphosphate hydrolase (GTPase) that localizes to recycling endosomes, and is most concentrated at the pericentriolar recycling compartment in a juxtanuclear distribution (Ren et al., 1998). Endogenous MTMR4 colocalized with the pericentriolar Rab11 (Fig. 2A, bottom panel, see arrow in high magnification image)

and partially with Rab11-decorated vesicles. Recombinant HA–MTMR4 colocalized in part with EEA1 (Fig. 2Ba), with the EEA1-derived PtdIns(3)P probe GFP–FYVE and with the early endosomal Rab5 GTPase (GFP–Rab5) (Fig. 2Bb,c). HA–MTMR4 colocalized partially with GFP–Rab5 and GFP–Rab4, particularly in the perinuclear region (supplementary material Fig. S2A,B). Using live-cell imaging, we also demonstrated that YFP–MTMR4 colocalized with Alexa Fluor 568–Tfn (A568–Tfn) within the first 5 minutes of Tfn loading, consistent with early endosomal localization (supplementary material Fig. S2C). However, HA–MTMR4 exhibited greater overlap with recycling endosomal markers, including GFP–Rab11, both in the perinuclear region and on vesicles (Fig. 2Bd). The exocyst component Sec15 is a recycling endosomal protein and interacts with Rab11 (Zhang et al., 2004). HA–MTMR4 exhibited significant colocalization with Xpress–Sec15 (Fig. 2Be).

Next, we evaluated the distribution of HA–MTMR4^{C407A} and revealed a similar colocalization as found for wild-type MTMR4, with partial colocalization with EEA1, recombinant GFP–FYVE and GFP–Rab5 (supplementary material Fig. S3A–C), but more significant colocalization with GFP–Rab11 (supplementary material Fig. S3D) and Xpress-tagged Sec15 (supplementary material Fig. S2E). HA–MTMR4 (supplementary material Fig. S2E) and HA–MTMR4^{C407A} (not shown) did not colocalize with the tagged

mannose 6-phosphate receptor (GFP–M6PR), which traffics between the Golgi and late endosomes (supplementary material Fig. S2E), or with the Golgi-resident proteins p230grip and TGN-46 (not shown). Thus, MTMR4 is found on both early and recycling endosomes. HA–MTMR4 also exhibited some colocalization with late endosomal markers such as LAMP-2 (supplementary material Fig. S2D).

The relative distribution of MTMR4 to early and recycling endosomes was determined by analysis of the degree of colocalization of HA–MTMR4 or HA–MTMR4^{C407A} with endogenous EEA1 and with the PtdIns(3)P probes GFP–FYVE (derived from EEA1) and 2×FYVE (derived from the endosomal protein Hrs), versus colocalization with GFP–Rab11 (Fig. 2C). This analysis showed that ~20% of MTMR4- or MTMR4^{C407A}-positive vesicles colocalized with vesicles labelled with EEA1, GFP–FYVE or GFP–2×FYVE, and that 60% colocalized with GFP–Rab11-labelled compartments. Therefore, MTMR4 might localize at the interface of the peripheral early endosome and the Rab11-enriched recycling compartment.

Constructs encoding individual domains for the MTMR4 PH, FYVE or CC+FYVE domains versus MTMR4 mutants lacking the PH (ΔPH) or FYVE (ΔFYVE) domains were generated and expressed intact in COS1 cells (supplementary material Fig. S4). The PH domain localized diffusely in the cytosol, the plasma membrane, the nucleus and actin stress fibres, colocalizing at this latter site with phalloidin-stained F-actin (supplementary material Fig. S5A). MTMR4 (ΔPH) localized to enlarged 'ring like' vesicles (supplementary material Fig. S5B). Therefore, the PH domain does not mediate endosomal localization on its own. HA–FYVE labelled the plasma membrane, cytosol and nucleus, and was detected only faintly on cytosolic vesicles (supplementary material Fig. S5C). HA–CC+FYVE localized intensely to endosomal vesicles, suggesting that both the coiled-coil and FYVE domains are required for efficient MTMR4 targeting to endosomes (supplementary material Fig. S5D). However, this construct did not colocalize with EEA1-positive endosomes or Rab11-positive endosomes at the pericentriolar compartment (supplementary material Fig. S5D). HA–ΔFYVE localized in a perinuclear distribution to a compartment displaying some tubularization, which overlapped intensely with Rab11 staining, consistent with the contention that the pericentriolar targeting domain lies outside the FVYE domain (supplementary material Fig. S5E). Therefore, no individual domain targets MTMR4 to early or recycling endosomes, rather multiple domains (including the FYVE and coiled-coil domains) contribute to MTMR4 endosomal localization.

Rab5 regulates endosome motility, early endosome fusion and clathrin-coated vesicle formation (Lawe et al., 2002; Smythe, 2002). Interestingly, rapalogue-induced MTM1 recruitment to Rab5-positive endosomes, but not expression of untargeted MTM1, leads to significant early endosomal tubularization (Fili et al., 2006). To determine whether MTMR4 could regulate Rab5-endosomal tubularization, we monitored GFP–Rab5-decorated endosomes in live cells using time-lapse imaging (not shown). However, no change in the morphology of Rab5-positive endosomes was detected in cells overexpressing MTMR4, which suggests that MTMR4 is either not sufficiently directed to Rab5-positive endosomes, and/or was not overexpressed at sufficiently high levels. Overexpression of the GTPase-deficient Rab5 mutant, Rab5Q79L, leads to the enlargement of early endosomes, resulting from enhanced homo- and heterotypic fusion (Barbieri et al., 1996). We noted that when Rab5Q79L was expressed, HA–MTMR4, and
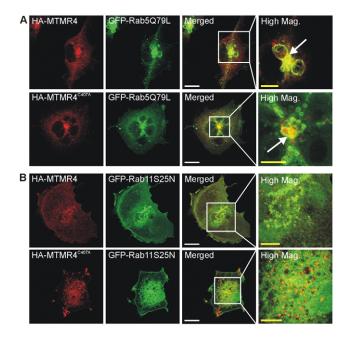

Fig. 3. MTMR4 localization is dependent on Rab5 and Rab11. COS1 cells were co-transfected with HA–MTMR4 or HA–MTMR4^{C407A} plus GFP–Rab5Q79L (**A**) or GFP–Rab11S25N (**B**), immunostained with HA antibodies and then visualized by confocal microscopy. High magnification images are shown on far right. Arrow indicates colocalization. White scale bars: 20 μm, yellow scale bars: 10 μm.

HA–MTMR4^{C407A} exhibited colocalization with dilated early endosomes (Fig. 3A).

Rab11S25N is a GDP-locked mutant that localizes to the cytosol rather than to recycling endosomes, as GTP hydrolysis is required for the recruitment of Rab11 and its effectors to endosomal membranes (Wilcke et al., 2000). In cells overexpressing Rab11S25N, HA–MTMR4 and HA–MTMR4^{C407A} exhibited more cytosolic localization with decreased perinuclear endosomal localization, suggesting that MTMR4 is recruited in part to recycling endosomes by active Rab11 (Fig. 3B). The recycling endosomal compartment is involved in receptor and lipid recycling (Hopkins and Trowbridge, 1983; Nichols et al., 2001) and is clustered around the centrosome, in a pericentriolar distribution, where in many cells it is tightly associated with the microtubule organising centre (MTOC) (Maxfield and McGraw, 2004). We noted that, following nocodozole treatment, the MTOC collapsed and microtubules dispersed, as demonstrated by co-staining with anti-β-tubulin (not shown). This result correlates with cytosolic redistribution of HA–MTMR4- and HA–MTMR4^{C407A}-decorated vesicles away from the perinuclear pericentriolar area (supplementary material Fig. S6). In control untreated cells, MTMR4 perinuclear staining overlapped tubulin staining of the MTOC (not shown). These results are consistent with the contention that MTMR4 localizes to microtubule-tethered vesicles that interface between early endosomes and the pericentriolar recycling endosomal network.

MTMR4 regulates the number of PtdIns(3)P-decorated endosomes

MTM1 regulates PtdIns(3)P levels on early endosomes, and MTMR2 degrades PtdIns(3)P on late endosomes (Cao et al., 2008).

We next examined whether MTMR4 regulates PtdIns(3)P levels and/or distribution on early or recycling endosomes. We used two experimental approaches to investigate this issue, both generating complementary findings. COS1 cells overexpressing wild-type or inactive MTMR4, or HeLa cells with siRNA–MTMR4 knockdown were fixed, digitonin-permeabilized and probed with recombinant purified GST–2×FYVE to detect PtdIns(3)P as described (Gillooly et al., 2000). HA–MTMR4 decreased the total cell PtdIns(3)P (by ~25%), relative to adjacent mock-transfected cells (Fig. 4A,C). By contrast, MTMR4^{C407A} increased total cell GST–2×FYVE staining by ~1.4-fold (Fig. 4A,C). At higher magnification, we noted an increase in the number of GST–2×FYVE-labelled vesicles (Fig. 4A, lower panel, far right) in MTMR4^{C407A}-expressing cells. Interestingly, under these conditions we could only show colocalization of GST–2×FYVE-decorated vesicles with EEA1-positive early endosomes, but not with GFP–Rab11-labelled recycling endosomes (Fig. 4B). In addition, not all EEA1-positive vesicles exhibited PtdIns(3)P colocalization, consistent with reports that PtdIns(3)P is required for EEA1 recruitment, but not its maintenance on endosomes (Fili et al., 2006).

HeLa cells were transiently transfected with siRNA oligonucleotides directed towards MTMR4, or with a negative control sequence (control siRNA). About 60% knockdown of MTMR4 was demonstrated by RT-PCR analysis (Fig. 4D). MTMR4 knockdown had no discernible effect on early endosome morphology, as assessed by EEA1 staining (Fig. 4E, lower left panel). The total cellular fluorescence of GST–2×FYVE staining, normalized to the cell area, was significantly increased in MTMR4 knockdown cells compared to control knockdown cells (Fig. 4F). Because similar increases in endosomal PtdIns(3)P levels were observed both in MTMR4 knockdown cells and following expression of MTMR4^{C407A}, it is probable that the latter construct functions as a dominant negative. We next evaluated whether the increased GST–2×FYVE staining in MTMR4 knockdown cells was due to an increase in PtdIns(3)P on each endosome and/or an increase in the number of PtdIns(3)P-decorated endosomes. The number of endosomes that were positive for GST–2×FYVE staining per cell, normalized to the cell area, was scored as a marker of PtdIns(3)P-positive endosomes and revealed a significant increase in MTMR4 knockdown cells (Fig. 4G). However, the average intensity of PtdIns(3)P per endosome, normalized to the endosome area, was not changed, as determined by the mean GST–2×FYVE fluorescence intensity per cell (Fig. 4H). These results suggest that MTMR4 controls PtdIns(3)P levels on a subset of endosomes. Under basal conditions, in which MTMR4 is expressed at normal levels, it is probable that this PtdIns(3)P pool is not be detectable using the experimental methods described here and that it is only upon expression of MTMR4 dominant-negative constructs, or following MTMR4 knockdown, that PtdIns(3)P on these endosomes becomes more apparent. We also demonstrated similar findings when cells expressing MTMR4 constructs or siRNA were co-transfected with GFP–FYVE and examined in either fixed cells by fluorescence microscopy or by live-cell imaging (not shown). In addition, there was no difference in the colocalization between PtdIns(3)P and Rab11-decorated vesicles, as detected in MTMR4 RNAi-depleted cells by GFP–Rab11 and mCherry–2×FYVE colocalization. Time-lapse imaging showed that approximately 10% of GFP–Rab11-labelled recycling endosomes transiently interacted with mCherry–2×FYVE, but this did not change following MTMR4 knockdown (not shown). Therefore, MTMR4 regulates PtdIns(3)P on a subset of endosomes.

MTMR4 regulates Tfn sorting into recycling endosomes

Recycling of Tfn or lipids that have passed through early/sorting endosomes can occur either via a fast pathway or through a second compartment (Rab11-positive perinuclear recycling endosomes) in a slower cycle (Hopkins et al., 1994; Sheff et al., 1999; Hao and Maxfield, 2000; Sheff et al., 2002). PI3K inhibition using wortmannin does not impair Tfn internalization; however, Tfn recycling is significantly reduced (Martys et al., 1996; Shpetner et al., 1996; Spiro et al., 1996). The bulk of Tfn returns rapidly from the early endosome to the plasma membrane in a PI3K-dependent manner via the fast pathway (Hunyady et al., 2002; van Dam et al., 2002; Zhao and Keen, 2008). Although the recycling of the Tfn-R has been characterized extensively, the molecular mechanisms that regulate receptor trafficking through early and recycling endosomes are still emerging (Brown et al., 1995; Gaullier et al., 1999; Odorizzi et al., 2000; Sonnichsen et al., 2000; van Dam and Stoorvogel, 2002). Because MTMR4 associates with both early and recycling endosomes, we examined the recycling of Tfn-R in cells with altered MTMR4 expression using Texas-Red-labelled Tfn (TR–Tfn) uptake and pulse-chase experiments as described (Simpson et al., 2004). After 5 minutes of uptake, TR–Tfn localized to vesicles scattered throughout the cytoplasm in both empty vector and MTMR4-expressing cells, suggesting that MTMR4 does not regulate Tfn uptake. In vector controls, TR–Tfn localized in a perinuclear distribution after 20 minutes chase, but by 40 minutes only a faint signal was evident, which indicates its clearance from the cell (Fig. 5A). HA–MTMR4 expression increased TR–Tfn accumulation in vesicles and in the perinuclear area at 20 minutes, which was still apparent at the 40 minute chase period. By contrast, in cells expressing HA–MTMR4^{C407}, Tfn rapidly cleared within 40 minutes (Fig. 5A). The related homologue, MTMR3, did not affect Tfn recycling, which suggests a unique function for MTMR4 (Fig. 5A). Internalized Tfn was quantified over a 90 minute pulse chase, revealing that MTMR4 significantly inhibited Tfn recycling, whereas MTMR3 had no effect (Fig. 5A,B). To examine whether HA–MTMR4^{C407A} acts as a dominant-negative construct, shorter time courses were evaluated. At 5 and 10 minutes, HA–MTMR4^{C407A}-expressing cells showed significantly less Tfn in the cell relative to vector-controls, suggesting accelerated recycling, (Fig. 5C). Interestingly, expression of various truncation mutants of MTMR4, which do not localize as wild-type MTMR4, (supplementary material Figs S4 and S5) did not significantly alter Tfn recycling, suggesting that the correct localization of MTMR4 is required for its function (Fig. 5D).

We also examined Tfn trafficking in MTMR4 siRNA HeLa cells using fluorescently labelled Tfn uptake, or using biotinylated transferrin (biotin–Tfn) together with avidin/horse radish peroxidise blot analysis (see Materials and Methods) (supplementary material Fig. S7). Under steady-state conditions, in cells treated with MTMR4 siRNA but not with control siRNA, Tfn loading into the cell was reduced by ~20% as assessed by immunofluorescence or by analysis of biotin–Tfn, although this was not statistically significant using biotin–Tfn (supplementary material Fig. S7A). The decrease in cellular Tfn loading at steady state in MTMR4 knockdown cells was specific for the clathrin-mediated endocytic pathway because we detected no alteration of the loading of the fluid phase marker dextran, a process that includes macropinocytosis (supplementary material Fig. S7B). PI3K activity is required for Tfn recycling but not for Tfn uptake into cells (Martys et al., 1996; Shpetner et al., 1996; Spiro et al., 1996). The decreased Tfn loading was corrected by inhibition of
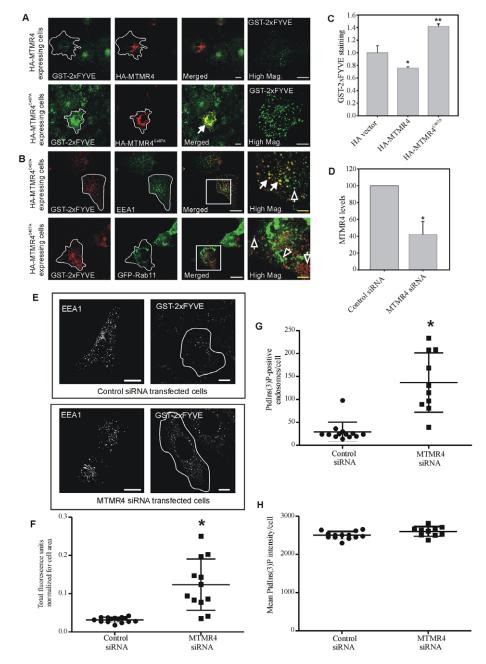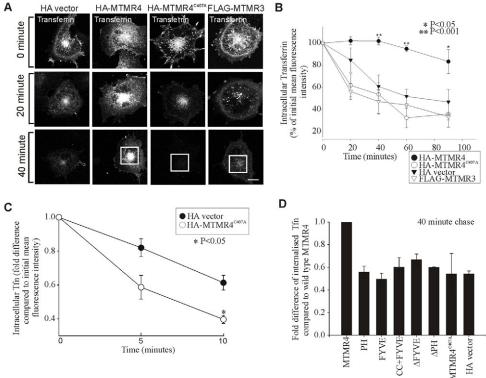
Fig. 4. MTMR4 regulates the number of PtdIns(3)P-decorated endosomes. (A) COS1 cells expressing HA–MTMR4 (top panel) or HA–MTMR4^{C407A} (bottom panel) were probed with recombinant GST–2×FYVE protein and stained with GST and HA antibodies, and visualized using confocal microscopy. Transfected cells (white outline) were compared to mock-transfected cells in the same field. High magnification images are shown on the far right. White scale bars: 20 µm, yellow scale bars: 10 µm. (B) COS1 cells expressing HA–MTMR4^{C407A} and co-transfected with GFP–Rab11 (bottom panel), were probed with GST–2×FYVE and stained with EEA1 (top panel), HA and GST antibodies. Transfected cells (white outline) were compared to mock-transfected cells in the same field. Solid arrows in high magnification images indicate colocalization; open arrows indicate independent localization. High magnification images of boxed areas are shown on far right. White scale bars: 20 µm, yellow scale bars: 10 µm. (C) COS1 cells expressing HA–vector, HA–MTMR4 or HA–MTMR4^{C407A} were stained as in A. GST–2×FYVE staining was expressed as the ratio of cellular fluorescence relative to adjacent mock-transfected cells in the same visual field. Results represent one representative experiment of three independent experiments in which n=15–20 cells were scored (*$P<0.05$, **$P<0.01$). (D) RNA from HeLa cells expressing MTMR4 siRNA oligonucleotides or control sequence (Control siRNA) was used as a template for quantitative RT-PCR. The percentage *MTMR4* mRNA levels amplified were compared to those for control siRNA-transfected cells (taken as 100%) ± s.e.m., determined for three independent experiments (*$P<0.05$). (E) HeLa cells expressing MTMR4 siRNA or control siRNA were stained with EEA1 antibodies (left panel), or GST–2×FYVE and GST antibodies (right panel) and visualized using confocal microscopy. Scale bars: 20 µm. (F) Total PtdIns(3)P per cell was quantified by measuring total GST–2×FYVE staining in the endosomes of each cell as the fluorescent signal above a selected threshold. Results represent total cellular GST–2×FYVE per cell and are normalized for total cell area (*$P<0.0001$). (G) The number of PtdIns(3)P-positive endosomes per cell was determined by automated image analysis as described in Materials and Methods. Results were normalized for cellular area (*$P<0.0001$). (H) The mean GST–2×FYVE staining intensity per cell was determined as the total endosomal fluorescence divided by endosomal area, and the results normalized to the mean GST–2×FYVE staining of control siRNA-expressing cells. Results represent one of two experiments. Error bars are mean ± s.d.; n=12–15 cells for each condition in that experiment.

Fig. 5. MTMR4 expression inhibits recycling of Tfn. (**A**) COS1 cells were co-transfected with Xpress–Tfn-R plus HA–vector, HA–MTMR4, HA–MTMR4^{C407A} or FLAG–MTMR3, pulsed with TR–Tfn (20 μg/ml) for 50 minutes and then incubated with unlabelled holo-Tfn (0.2 mg/ml) for the indicated times. Cells were then washed and immunostained with HA antibodies to identify transfected cells and visualized by confocal microscopy. All images were obtained using the same laser attenuation. The white boxes highlight internalized TR–Tfn. Scale bar: 20 μm. (**B**) Tfn recycling assays were repeated as in A. Internalized Tfn was quantified using ImageJ. Results represent the mean ± s.e.m. for 20 cells per condition for three independent experiments. (**C**) Tfn recycling assays were repeated as in A, and Tfn quantified at 5 and 10 minute chase in cells expressing HA–vector or HA–MTMR4^{C407A}. Results represent the mean ± s.e.m. of 20 cells per condition for three independent experiments. (**D**) COS1 cells were transiently co-transfected with Xpress–Tfn-R plus HA–MTMR4, HA–PH, HA–FYVE, HA–CC+FYVE, HA–ΔFYVE, HA–ΔPH, HA–MTMR4^{C407A} or HA–vector alone. Tfn recycling assays were repeated as in A for a 40 minute chase. Results represent the mean ± s.e.m. for 20 cells per condition for three independent experiments. Results are expressed relative to wild-type MTMR4.

PI3K activity by LY294002 treatment, suggesting subtle changes in recycling of Tfn in MTMR4 knockdown cells under steady-state conditions (supplementary material Fig. S7C). However, analysis of the recycling of Tfn by pulse-chase experiments by either live-cell imaging of fluorescently labelled Tfn (supplementary material Fig. S7D, left panel), or by biotin–Tfn avidin/horse radish peroxidise blots (Fig. S7D, right panel), showed no significant differences between MTMR4 and control knockdown cells. Therefore, knockdown of MTMR4 alone is insufficient to regulate Tfn recycling from early endosomes to the plasma membrane, and other MTMs might contribute, given that expression of the dominant-negative MTMR4 construct results in accelerated Tfn recycling. Changes in Tfn loading at steady state could be caused by changes in Tfn-R expression on the cell surface or by changes in total cellular receptor levels. However, no difference in the levels of Tfn-R on the surface of MTMR4 siRNA cells as compared with control siRNA cells was apparent when surface receptor levels were assessed (supplementary material Fig. S8, middle panel). Immunoblot analysis revealed a 20% reduction in the total cellular levels of the receptor; however, this was not statistically significant (supplementary material Fig. S8, lower panel).

To evaluate whether MTMR4 expression regulates Tfn transit from early endosomes, we colocalized internalized TR–Tfn with EEA1. In vector controls at early time points, TR–Tfn was concentrated in early endosomes, as shown by its colocalization with EEA1. However, after a 10 minute chase TR–Tfn exited this compartment (Fig. 6A, left panels and Fig. 6B). By contrast, ~75% of vesicles were positive for both EEA1 and TR–Tfn for the entire 90 minute chase period in MTMR4-expressing cells (Fig. 6A, right panels and Fig. 6B). Therefore, MTMR4 regulates the exit of cargo from early endosomes into recycling pathways.

We also examined the distribution of Tfn-R, a marker of peripheral early and perinuclear recycling endosomes, in cells overexpressing MTMR4. Cells were co-transfected with Xpress–Tfn-R and either HA–MTMR4 or empty vector, and then depleted of endogenous Tfn by serum-starvation. Pulse-chase experiments using TR–Tfn were then performed. Prior to the initiation of recycling (time zero), Xpress–Tfn-R exhibited a cytosolic and vesicular distribution regardless of the MTMR4 construct expressed (not shown). After 40 minutes recycling, Xpress–Tfn-R accumulated in the perinuclear recycling compartment and colocalized with TR–Tfn (Fig. 6C upper panels) in cells expressing empty vector. However, at the same time point, in cells expressing wild-type HA–MTMR4, we noted that TR–Tfn did not colocalize significantly with Tfn-R (Fig. 6C, lower panels) and that the receptor exhibited a more diffuse distribution. In addition, we noted a striking enlargement of HA–MTMR4-decorated vesicles
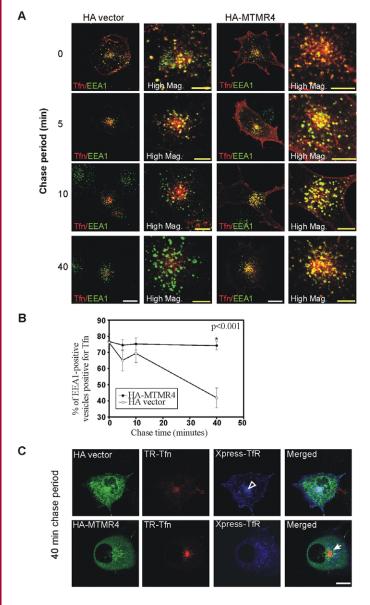
Fig. 6. MTMR4 delays Tfn exit from early endosomes. (A) COS1 cells were co-transfected with Xpress–Tfn-R and either HA–vector or HA–MTMR4, pulsed with TR–Tfn (20 μg/ml) for 50 minutes and then incubated with unlabelled holo-Tfn (0.2 mg/ml) for the indicated times. Cells were then washed and co-immunostained with EEA1 and HA antibodies and visualized by confocal microscopy. EEA1 (green) and TR–Tfn (red) are shown. High magnification images are shown on right. White scale bars: 20 μm, yellow scale bars: 10 μm. **(B)** Tfn recycling assays were repeated as in A, and the number of cells showing colocalization between EEA1 and Tfn scored at 5, 10 and 40 minutes. Results represent the mean ± s.e.m. of 20 cells per condition for three experiments. **(C)** COS1 cells expressing Xpress-tagged Tfn receptor and HA–vector (top panel), or HA–MTMR4 (lower panel) were pulsed with TR–Tfn (20 μg/ml) for 50 minutes, and incubated for 40 minutes with unlabelled holo-Tfn (0.2 mg/ml). Cells were fixed and stained with HA and Xpress antibodies. Arrowhead indicates Tfn-R in the perinuclear recycling compartment. Arrow indicates colocalization of HA–MTMR4 and Xpress–Tfn-R in merged image and dilatation of MTMR4 decorated endosomes.

(Fig. 6C, arrows), which colocalized with Xpress–Tfn-R in a subpopulation of vesicles. Therefore, MTMR4 regulates the trafficking of Tfn and its receptor through early endosomes.

MTMR4 expression affects the cellular distribution of recycling endosomes

Receptors can be recycled in two ways, either by a fast pathway via peripheral early endosomes marked with Rab4, or alternatively by a slow perinuclear recycling compartment marked with Rab11 (Daro et al., 1996; Ullrich et al., 1996; Sonnichsen et al., 2000). We next investigated whether MTMR4 altered the steady-state distribution of markers of the slow recycling endosomal compartment, which concentrate in the perinuclear Rab11-positive recycling compartment, by examining the distribution of GFP–Rab11 (Fig. 7). In MTMR4 RNAi knockdown cells we noted dispersal of the GFP–Rab11-positive recycling compartment from its normal juxtanuclear position into a larger more diffuse localization, suggesting its redistribution. The area of perinuclear GFP–Rab11 was evaluated relative to the nuclear area of the same cell, revealing a twofold increase in MTMR4 siRNA knockdown cells, relative to siRNA control cells (Fig. 7B). We also investigated whether MTMR4 expression regulated the tubulation of Rab11-positive vesicles, but could show no consistent differences when this was assessed in fixed cells, or by live-cell imaging in MTMR4 knockdown cells that coexpressed GFP–Rab11 (not shown).

VAMP3, also called cellubrevin (Ceb or Cb) (McMahon et al., 1993; Galli et al., 1994), is a vesicular (v-) R-SNARE protein that regulates the recycling of plasma membrane receptors, including Tfn-R and Glut-4 (Galli et al., 1994; Breton et al., 2000; Polgar et al., 2002; Borisovska et al., 2005; Murray et al., 2005). VAMP3 is enriched on recycling endosomes. GFP–VAMP3 has been used experimentally as a marker of trafficking from the endocytic recycling compartment to the plasma membrane (Galli et al., 1994; Breton et al., 2000; Polgar et al., 2002; Borisovska et al., 2005; Murray et al., 2005). To further analyse the role that MTMR4 plays in regulating the recycling compartment, GFP–VAMP3 was co-expressed with HA–vector, HA–MTMR4 or HA–MTMR4^{C407A}. In control studies, these experiments were also undertaken in cells expressing mCherry–p230grip, a Golgi marker. At all times, GFP–VAMP3 exhibited a distinct perinuclear localization to this Golgi marker (not shown), consistent with its localization to the pericentriolar recycling compartment. Cells were imaged live to evaluate GFP–VAMP3 distribution (Fig. 7C). In vector controls, GFP–VAMP3 was detected prominently in a perinuclear distribution, consistent with the endocytic recycling compartment, but was also detected on cytoplasmic vesicles (Fig. 7C, left hand panel). However, in cells expressing MTMR4, GFP–VAMP3 was confined to a perinuclear distribution, and cytoplasmic VAMP3-coated vesicles were less apparent (Fig. 7C, middle panel). By contrast, in cells expressing MTMR4^{C407A} (Fig. 7C, right hand panel), VAMP3 was more prominent on peripheral cytoplasmic vesicles with reduced perinuclear distribution, and at the plasma membrane (Fig. 7C, arrows). Interestingly, we noted a mild dilation of VAMP3-positive endosomes in cells expressing HA–MTMR4; however, this dilation was more profound in cells expressing HA–MTMR4^{C407A} (Fig. 7C, see arrowheads). Therefore, MTMR4 restrains the movement of the endocytic recycling compartment towards the cell periphery.

Discussion

Resident early endosomal PtdIns(3)P is required for the recycling of Tfn from the EEA1-positive endosomal compartment and its rapid return to the plasma membrane (van Dam et al., 2002). However, to date the lipid phosphatase that selectively regulates
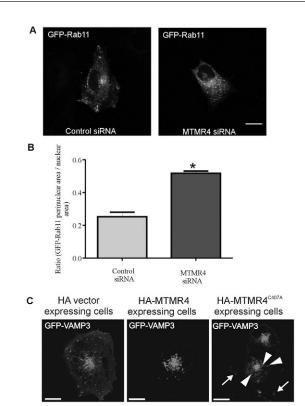
Fig. 7. MTMR4 regulates the distribution of the recycling endosomal compartment. (**A**) HeLa cells were transfected with MTMR4 siRNA or control siRNA and GFP–Rab11 and imaged live by confocal microscopy. Representative images are shown. (**B**) The relative perinuclear distribution of GFP–Rab11 was determined as described in Materials and Methods. Results shown are the means of three independent experiments and represent 27–34 cells analysed per transfection. (*$P<0.005$); error bars indicate s.e.m. (**C**) COS1 cells expressing GFP–VAMP3 plus HA–vector, HA–MTMR4 or HA–MTMR4^{C407A} were imaged live by wide-field microscopy, and GFP–VAMP3 observed. Arrows indicate plasma membrane GFP–VAMP3 distribution. Arrowheads indicate dilated endosomes. Scale bars: 20 μm.

this pool of PtdIns(3)P has not been identified. This study shows that MTMR4 localizes to both early and recycling endosomes and regulates the exit of Tfn into recycling pathways. In cells overexpressing MTMR4, the recycling of Tfn was severely impaired and Tfn was trapped in early endosomes. Furthermore, MTMR4 also regulated the distribution of the endocytic recycling compartment. MTMR4 expression or knockdown resulted in redistribution of Rab11- and VAMP3-decorated endosomes. Therefore, the study reported here identifies MTMR4 as a novel regulator of endosomal sorting from early endosomes into recycling pathways.

Several previous studies have localized recombinant MTMR4, with one report describing its localization to early endosomes when overexpressed in HeLa cells (Lorenzo et al., 2006). A recent study described MTMR4 in complex with Nedd4, and recombinant MTMR4 colocalization with Rab7 and Tfn (Plant et al., 2009). We have demonstrated here that both endogenous and recombinant MTMR4 localize to early endosomes, and have also revealed the novel findings that MTMR4 also decorates recycling endosomes and concentrates in the juxtanuclear recycling compartment. Tfn-enriched vesicles interact only transiently with EEA1-decorated endosomes, in contrast to EGF, which is incorporated and retained

in EEA1-decorated endosomes (Leonard et al., 2008). Tfn-containing vesicles rapidly disassociate from early endosomes and localize to a juxtanuclear compartment, the site at which we detect the highest MTMR4 localization.

PtdIns(3)P is required for early endosome fusion, motility of vesicles along microtubules and Tfn recycling (Gorvel et al., 1991; McBride et al., 1999; Nielsen et al., 1999; van Dam et al., 2002). Several studies have shown that the MTM phosphatases control only a modest 10–20% of PtdIns(3)P total cellular levels, on the basis of overexpression studies using MTM1 (Taylor et al., 2000; Tronchere et al., 2004). Moreover, examination of three myoblast cell lines derived from individuals with X-linked myotubular myopathy, a genetic disorder in which MTM1 is mutated, revealed no detectable differences in endosomal PtdIns(3)P using the GST–2×FYVE probe (Biancalana et al., 2003; Tronchere et al., 2004). Distinct MTMs might concentrate at discrete subcellular sites to degrade PtdIns(3)P on specific microdomains within the endosomal network, rather than degrade the total cellular levels of PtdIns(3)P levels per se (Laporte et al., 1996; Taylor et al., 2000; Tronchere et al., 2004). We have shown here that MTMR4 expression decreased PtdIns(3)P levels on endosomes. Conversely, MTMR4 siRNA knockdown or dominant-negative MTMR4 expression increased the number of PtdIns(3)P-decorated endosomes, rather than increasing the level of PtdIns(3)P on each endosome. Therefore, MTMR4 might control PtdIns(3)P levels on a subset of endosomes that regulate Tfn exit from early endosomes into recycling pathways, and that might express PtdIns(3)P at very low levels that are beyond the limits of current experimental detection.

Despite the localization of MTMR4 to recycling endosomes and an increase in PtdIns(3)P-decorated vesicles in MTMR4 knockdown cells or following expression of dominant-negative MTMR4, the majority of PtdIns(3)P-decorated endosomes showed colocalization with EEA1, but not Rab11. There is little evidence that PtdIns(3)P localizes to or functions at the pericentriolar juxtanuclear recycling compartment (Gillooly et al., 2000). PtdIns(3)P might be expressed at low levels on recycling endosomes, beyond the limits of detection of current experimental techniques. We could find only one report of PtdIns(3)P localization on Rab11-positive endosomes, albeit at low levels (Shin et al., 2005). In the Shin et al. study, approximately 20% of Rab11-positive endosomes showed overlap with GFP–2×FYVE staining, used as a marker for PtdIns(3)P; however, these endosomes were also positive for Rab4, which suggests that they represent sorting endosomes. This is consistent with our observations that in HeLa cells ~10% of Rab11-positive endosomes interacted with PtdIns(3)P-decorated endosomes. Although early endosomes and the sorting and recycling endosomes have distinct functions, the transition from one to another can overlap and this could include the transition of PtdIns(3)P-decorated early endosomes to sorting and recycling endosomes.

The progression from Rab5- to Rab4- to Rab11-positive endosomes is required for Tfn-R and Tfn recycling (Sonnichsen et al., 2000). At steady state, internalized Tfn resides in early endosomes and the endocytic recycling compartment occupying a juxtanuclear position in many cells (Maxfield and McGraw, 2004). Targeting of MTM1 to Rab5-enriched early endosomes results in extensive tubulation of Rab5-positive endosomes and delayed the exit of Tfn from early endosomes (Fili et al., 2006), although whether endogenous MTM1 functions to regulate these events is unknown. As reported here, expression of wild-type MTMR4

arrested Tfn sorting in early endosomes, correlating with reduced early endosomal PtdIns(3)P. However, our studies (unlike those reported using Rab-5 directed MTM1) did not require specific targeting of MTMR4 to endosomes. Therefore, by regulating a specific pool of PtdIns(3)P on early endosomes, MTMR4 might control the entry of Tfn into the recycling pathway. Consistent with this, we noted that under steady-state conditions the total levels of Tfn in MTMR4 knockdown cells was slightly decreased (~20%). This phenotype was corrected by PI3K inhibition, suggesting accelerated recycling in these cells. However, we were unable to demonstrate using pulse-chase experiments that MTMR4 knockdown affected Tfn recycling, despite observations that dominant-negative MTMR4 accelerated recycling. These results suggest that other MTMs might contribute with MTMR4 to regulating Tfn recycling, or that the degree of knockdown of MTMR4 that we were able to achieve (~60%) was insufficient to negate all MTMR4 function.

To further investigate the recycling endosomal network, we examined Rab11 and VAMP3 distribution. There is some evidence that the endocytic recycling compartment provides a local pool of intracellular receptors for rapid delivery to the cell surface (Szekeres et al., 1998; Lin et al., 2000; Park et al., 2004). For example, Rab11 regulates protein transport from the endocytic recycling compartment to the trans-Golgi network and the plasma membrane (Wilcke et al., 2000). We noted a redistribution of Rab11-decorated endosomes from the juxtanuclear recycling compartment in MTMR4 siRNA-depleted cells, which suggests that MTMR4 affects either the entry of Rab11-positive vesicles from sorting endosomes into the endocytic recycling compartment or, alternatively, that it regulates the exit. Expression of dominant-negative MTMR4 was associated with the redistribution of GFP–VAMP3 from the endocytic recycling compartment, whereas overexpression of MTMR4 inhibited release. This is consistent with the contention that this lipid phosphatase regulates the intracellular distribution of the recycling compartment. MTMR4 degradation of PtdIns(3)P might regulate vesicle motility and/or fusion, by reducing effector recruitment to endosomes. Following MTMR4 knockdown or upon expression of dominant-negative MTMR4, our results suggest that localized increases in PtdIns(3)P might drive endosomes to the cell periphery away from the pericentriolar recycling compartment.

Similar to the other MTMs, we have shown here that MTMR4 hydrolyses PtdIns(3,5)P_2 to form PtdIns(5)P. However, it seems unlikely that MTMR4 degradation of PtdIns(3,5)P_2 regulates Tfn sorting. Expression of dominant-negative PIKfyve^{K1831E}, or PIKfyve protein knockdown in mammalian cells, does not affect receptor internalization, Tfn recycling or receptor trafficking to lysosomes (Ikonomov et al., 2003; Rutherford et al., 2006). In mammalian cells, PIKfyve RNAi-mediated knockdown impairs early endosome-to-TGN traffic and potentiates exocytosis of neurosecretory vesicles (Rutherford et al., 2006; Osborne et al., 2008). However, we found that MTMR4 expression did not alter retrograde trafficking from early endosomes to the Golgi, as shown by the normal retrograde trafficking of cholera toxin from early endosomes to the Golgi (see supplementary material Fig. S9). Furthermore, MTMR4 expression did not alter the subcellular distribution of mannose 6-phosphate receptor and/or its levels.

In summary, this study has identified a lipid phosphatase, MTMR4, that contributes to cargo selection for recycling, revealing specificity in MTMR4 localization in relation to its function at the interface between early and recycling endosomes.

Materials and Methods

General reagents and vectors

Restriction and DNA-modifying enzymes were from New England Biolabs (Beverly, MA), Fermentas (Hanover, MD), or Promega (Madison, WI). GFP–FYVE (EEA1) and GST–2×FYVE (Hrs) were from Tamas Balla (Endocrinology and Reproduction Research Branch, NICHD, Bethesda, MD) and Tadaomi Takenawa (Department of Biochemistry, Institute of Medical Science, University of Tokyo, Japan); mCherry–2×FYVE (Hrs) from Harald Stenmark (Institute for Cancer Research, Oslo, Norway); GFP–Rab11, Xpress–Rab11S25N, Xpress–Sec15 and Xpress–Tfn-R from Tony Rowe (Biogenidec, San Diego, CA), mCherry–p230grip from Paul Gleeson (Bio21 Institute, Melbourne University, Australia), GFP–M6PR from Jeffrey Pessin (Pharmacological Sciences, Stony Brook University, New York); YFP–MTMR4, FLAG–MTMR3, from Jocelyn Laporte (IGBMC-INSERM, University of Louis Pasteur de Strasbourg, France); GFP–Rab4 from Volker Haucke (Institute of Chemistry and Biochemistry, Freie Universitaet Berlin, Germany). TR–Tfn, A568–Tfn and FITC-cholera toxin were from Molecular Probes. Other reagents were from Sigma-Aldrich (St Louis, MO).

Mammalian expression plasmids

Full-length MTMR4 cDNA was amplified from pcDNA3 vector (a gift from Runxiang Zhao, Department of Medicine, Vanderbilt University, Nashville, TN) and cloned into the $Kpn1$ site of HA-tagged mammalian expression vector pCGN. The MTMR4^{C407A} construct was generated by site-directed mutagenesis (Quickchange, Stratagene). The MTMR4 PH domain (amino acids 25–125), FYVE domain (amino acids 1109–1175), CC+FYVE (amino acids 1022–1175), ΔPH (amino acids 125–1175) and ΔFYVE (amino acids 1–1109) constructs were generated by PCR amplification, and subcloned into pCGN. Correct insertion into vector, and fidelity of insert sequence was confirmed by Big-Dye Terminator DNA sequencing.

Antibodies and protein expression

Two New Zealand White rabbits were immunized with the MTMR4 peptide (^{1092}CLEASWEPVDKKETE^{1107}C) conjugated via the terminal cysteine to diphtheria toxoid. Serum was purified on an immunopeptide-coupled thiopropyl-Sepharose 6B resin. Monoclonal β-tubulin and Xpress antibodies were from Invitrogen. Other products used were monoclonal HA antibody (Silenus, Melbourne, Australia); polyclonal HA antibody (Clontech, CA); monoclonal FLAG antibody (Sigma); polyclonal GST antibody, anti-Tfn-R and Rab11 antibody (Zymed Laboratories, South San Francisco, CA); phalloidin and Alexa-Fluor-488-conjugated and Alexa-Fluor-594-conjugated secondary antibodies (Molecular Probes, Eugene, OR); mouse early endosomal antigen (EEA1) antibody (Cytostore, Calgary); and anti-CD71 (BD Pharmingen). Recombinant GST–2×FYVE protein was expressed and purified as described (Furutani et al., 2006). Cell lysates for immunoblot analysis were harvested in 50 mM Tris pH 8, 150 mM NaCl, 1% Triton X-100, 2 mM EDTA, 1 mM benzamadine, 2 mM phenylmethylsulfonylfluoride, 2 μg/ml leupeptin and 2 μg/ml aprotinin for 1 hour, and pelleted by centrifugation into Triton-soluble and Triton-insoluble fractions.

Cell culture, transient transfections, microscopy and image analysis

COS1 and HeLa cells were cultured in Dulbecco's modified Eagle's medium (DMEM), with 100 U/ml penicillin/streptomycin, 2 mM glutamine and either 5% or 10% fetal calf serum (FCS) (CSL Biosciences, Parkville, Australia), respectively, and transfected using DEAE–dextran chloroquine. HeLa cells were transfected with Fugene 6 reagent (Roche, Switzerland) or lipofectamine LTX (Invitrogen). For confocal microscopy, transfected cells were grown on coverslips and allowed to recover for 24–48 hours, fixed with 3% paraformaldehyde, permeabilized with 0.1% Triton X-100, and blocked in 1% BSA (in PBS). Monoclonal anti-HA (1:1000), polyclonal HA (1:200), anti-EEA1 (1:50), anti-Xpress (1:1000), anti-Rab11 (1:20), and anti-MTMR4 (1:10) were incubated for 1 hour at room temperature (RT). GST–2×FYVE staining was an adaptation of a published method (Gillooly et al., 2000). Cells were fixed with 3% PFA (10 minutes), permeabilized with 40 μg/ml digitonin in 3% BSA (30 minutes), blocked (30 minutes) in 3% BSA, and incubated with 5 μg/ml GST–2×FYVE in 3% BSA (30 minutes). After washing, cells were stained with GST antibodies and Alexa-Fluor-488-conjugated and Alexa-Fluor-594-conjugated secondary antibodies (1:700). Coverslips were washed three times with PBS and mounted onto glass slides by using Slowfade Gold reagent (Invitrogen). Single-plane or stacked images were obtained using a Leica TCS-NT Krypton confocal microscope and a 40× oil (NA 0.85) or 100× oil (NA1.4) immersion objective.

Live-cell imaging was conducted on a wide-field Leica AF6000LX system using a 63× water objective (NA 1.2) or an Olympus FV1000 confocal microscope using 100× oil immersion objective (NA 1.4), or on a Leica SP5 confocal microscope using 40× oil objective (NA 1.25). Immediately before the experiment, medium was replaced with DMEM supplemented with 25 mM HEPES and 0.5 g/l bicarbonate, pH 7.4. Cells were maintained at 37°C and imaged over the time-course in a 5% CO_2 humidified chamber at 37°C.

Single-plane confocal images were analysed using AnalySIS software (Olympus Soft Imaging). The thresholded MTMR4-positive pixels that colocalized with the thresholded pixels of each marker protein were quantified and represented as the percentage of total MTMR4 pixels. All pixels with intensity above 100 were counted from a 0–255 8-bit image. Colocalization was detected as yellow (green + red) pixels

in the merged images. All other image analyses utilized ImageJ software (v1.41 ImageJ, US NIH, Bethesda, MD, http://rsb.info.nih.gov/ij/, 1997-2008).

Endosomal GST–2×FYVE signal was distinguished using the threshold function; within independent experiments a constant threshold was applied to both the knockdown and control conditions. Total and mean fluorescence values were recorded as the integrated density and mean of thresholded images, respectively. Images were converted to a binary image and watershed applied. The number of individual GST–2×FYVE endosomes per cell was determined using a cut-off particle size of 9 pixels (0.07 μm²). Total fluorescence and endosomal number per cell were normalized to the area per cell determined by freehand tracing of the cell boundary. Mean endosomal fluorescence was normalized to the area of the fluorescent endosomal signal within cells. The perinuclear distribution of GFP–Rab11 was examined live (AF6000LX) by imaging a Z-stack as maximum projection. The area of perinuclear signal boundaries was expressed as a ratio of the nuclear area.

RNAi knockdown of MTMR4
Validated MTMR4 RNA oligonucleotides (catalogue #AM51333/ID104747) or control sequence #1 (catalogue #AM4635) were labelled with Cy3 fluorophore (Ambion, Austin, TX). HeLa cells were transfected with 25 pmol siRNAs in 24-well, or 80 pmol in six-well dishes, using Lipofectamine 2000 (Invitrogen). In these experiments, the control sequence was All Stars (Qiagen). At 24 hours post-siRNA transfection, cells were transfected with DNA constructs. At 48 hours post-RNA transfection, cells were harvested or processed for immunofluorescence. RNA was extracted using the RNEASY Mini Kit (Qiagen) and used for RT-PCR (Quantitect Sybr Green RT-PCR kit, Qiagen) using *Hs* MTMR4 and GAPDH reference gene primers (Qiagen). The 20 μl reactions contained 2.5–4 ng/μl RNA and 20 pmol of each primer. Reactions were conducted in triplicate in a Rotorgene 3000 Real-Time PCR cycler (Corbett). Relative MTMR4 expression was calculated using the ΔΔCt method (Ct, cycle threshold) (Dussault and Pouliot, 2006).

Lipid phosphatase assays
Cells were lysed in 10 mM HEPES, 10 mM KCl, 0.1 mM EDTA, 1 mM DTT, 0.1 mm Na₃VO₄, and 0.2% NP-40, then incubated with HA antibodies (Covance) plus protein-A-coated Sepharose beads overnight at 4°C. Cells were then washed four times in 10 mM HEPES pH 8, 10 mM KCL, 0.1 mM EDTA, 0.2% NP-40, Roche complete mini protease cocktail inhibitor tablet, and then twice in 50 mM ammonium acetate, pH 6 and assayed using di-C8-NBD fluorescent phosphoinositides (Echelon Research Laboratories) according to Taylor and Dixon (Taylor and Dixon, 2004). Reaction products were resolved by thin layer chromatography on silica gel and visualized by UV light.

Tfn recycling assays
For immunofluorescence-based assays, COS1 cells were transfected with Xpress–Tfn-R and HA–MTMR4, HA–MTMR4^{C407A}, HA–vector or FLAG–MTMR3. At 24 hours post-transfection, cells were serum-starved overnight and incubated with 20 μg/ml TR–Tfn for 50 minutes at 37°C, washed three times with ice cold PBS, and then left on ice (0 time point) or incubated with chase medium containing 200 μg/ml of unlabelled human holo-Tfn at 37°C, as described (Lindsay and McCaffrey, 2002). At the indicated times, cells were washed three times with ice-cold PBS and then fixed. Laser attenuation settings were constant for all experiments. The mean (*n*=10–20 cells) fluorescence intensity was measured for each condition, and expressed as a percentage of the mean fluorescence intensity of cells fixed immediately after TR–Tfn internalization (time 0 minutes).

Live-cell imaging of Tfn recycling in HeLa cells treated with MTMR4 siRNA or control siRNA was performed on an SP5 confocal microscope. At 24 hours after siRNA application, cells were removed from 24-well dishes with trypsin and seeded onto 25-mm coverslips for an additional 24 hours. Cells were incubated in serum-free DMEM for 30 minutes, and then incubated for 60 minutes with media containing 2 μg/ml A568–Tfn. Prior to imaging, cells were chased with 200 mcg/ml holo-Tfn. Images were acquired every 2 minutes. Time series were analysed by encircling the perinuclear transferrin signal in individual cells at each time point and normalizing the fluorescent results for each cell with its baseline perinuclear signal.

Tfn recycling in MTMR4 knockdown cells was also determined using biotin–Tfn (10 μg/ml). Cells were incubated in serum-free DMEM for 30 minutes, and then incubated for 60 minutes with media containing biotin–Tfn, followed by wash and chase with holo-Tfn as above. Cells from each time point were collected and lysed in sample buffer for SDS-PAGE and transferred to nitrocellulose membranes. Blots were incubated for 30 minutes with avidin/horse radish peroxidise (ABC elite Vector Laboratories, Burlingame, CA), according to the manufacturer's instructions. The intensity of each biotin–Tfn-positive band was measured using ImageJ. Protein loading was controlled for by detection of β-tubulin. Data were represented as the fraction of retained Tfn. The zero-minute chase was set at 1.0.

Cholera toxin uptake assays
Fluorescent cholera toxin (FITC–Ctx) assays were a modification of experiments previously described (Bujny et al., 2007; Mesa et al., 2005). COS1 cells were transfected with HA–MTMR4 or HA–vector for 24 hours, pre-chilled at 4°C for 10 minutes, and then incubated for 30 minutes in uptake medium (serum-free DMEM, 0.5% BSA, 20 mM HEPES pH 7.2) containing 2 μg/ml FITC-Ctx at 4°C. Cells were

washed, incubated in uptake medium at 37°C, fixed at the indicated times and immunostained with anti-HA antibodies.

Statistical differences were calculated using two way Student's *t*-test for paired or unpaired data where indicated. All statistical analysis used GraphPad prism (v5.01 GraphPad Software).

References

Abe, N., Inoue, T., Galvez, T., Klein, L., Meyer, T. (2008). Dissecting the role of PtdIns(4,5)P₂ in endocytosis and recycling of the transferrin receptor. *J. Cell Sci.* **121**, 1488-1494.

Azzedine, H., Bolino, A., Taïeb, T., Birouk, M, Di Duca, A., Bouhouche, S. B. A., Mrabet, T., Hammadouche, T., Chkili, R. G. R., Ravazzolo Brice, A. et al. (2003). Mutations in MTMR13, a new pseudophosphatase homologue of MTMR2 and Sbf1, in two families with an autosomal recessive demyelinating form of Charcot-Marie-Tooth disease associated with early-onset glaucoma. *Am. J. Hum. Genet.* **72**, 1141-1153.

Barbieri, M. A., Li, G., Mayorga, L. S. and Stahl, P. D. (1996). Characterization of Rab5:Q79L-stimulated endosome fusion. *Arch. Biochem. Biophys.* **326**, 64.

Begley, M. J., Taylor, G. S., Kim, S.-A., Veine, D. M., Dixon, J. E. and Stuckey, J. A. (2003). Crystal structure of a phosphoinositide phosphatase, MTMR2: insights into myotubular myopathy and Charcot-Marie-Tooth syndrome. *Mol. Cell* **12**, 1391.

Berger, P., Bonneick, S., Willi, S., Wymann, M. and Suter, U. (2002). Loss of phosphatase activity in myotubularin-related protein 2 is associated with Charcot-Marie-Tooth disease type 4B1. *Hum. Mol. Genet.* **11**, 1569-1579.

Berger, P., Berger, I., Schaffitzel, C., Tersar, K., Volkmer, B. and Suter, U. (2006). Multi-level regulation of myotubularin-related protein-2 (mtmr2) phosphatase activity by myotubularin-related protein-13/set-binding factor-2 (MTMR13/SBF2). *Hum. Mol. Genet.* **15**, 569-579.

Biancalana, V., Caron, O., Gallati, S., Baas, F., Kress, W., Novelli, G., D'Apice, M. R., Lagier-Tourenne, C., Buj-Bello, A., Romero, N. B. et al. (2003). Characterisation of mutations in 77 patients with X-linked myotubular myopathy, including a family with a very mild phenotype. *Hum. Genet.* **112**, 135-142.

Blondeau, F., Laporte, J., Bodin, S., Superti-Furga, G., Payrastre, B. and Mandel, J.-L. (2000). Myotubularin, a phosphatase deficient in myotubular myopathy, acts on phosphatidylinositol 3-kinase and phosphatidylinositol 3-phosphate pathway. *Hum. Mol. Genet.* **9**, 2223-2229.

Bolino, A., Muglia, M., Conforti, F. L., LeGuern, E., Salih, M. A., Georgiou, D. M., Christodoulou, K., Hausmanowa-Petrusewicz, I., Mandich, P., Schenone, A. et al. (2000). Charcot-Marie-Tooth type 4B is caused by mutations in the gene encoding myotubularin-related protein-2. *Nat. Genet.* **25**, 17-19.

Borisovska, M., Zhao, Y., Tsytsyura, Y., Glyvuk, N., Takamori, S., Matti, U., Rettig, J., Sudhof, T. and Bruns, D. (2005). v-SNAREs control exocytosis of vesicles from priming to fusion. *EMBO J.* **24**, 2114-2126.

Breton, S., Nsumu, N. N., Galli, T., Sabolic, I., Smith, P. J. S. and Brown, D. (2000). Tetanus toxin-mediated cleavage of cellubrevin inhibits proton secretion in the male reproductive tract. *Am. J. Physiol. Renal Physiol.* **278**, F717-F725.

Brown, W., DeWald, D., Emr, S., Plutner, H. and Balch, W. (1995). Role for phosphatidylinositol 3-kinase in the sorting and transport of newly synthesized lysosomal enzymes in mammalian cells. *J. Cell Biol.* **130**, 781-796.

Bujny, M. V., Popoff, V., Johannes, L. and Cullen, P. J. (2007). The retromer component sorting nexin-1 is required for efficient retrograde transport of Shiga toxin from early endosome to the trans golgi network. *J. Cell Sci.* **120**, 2010-2021.

Cao, C., Laporte, J., Backer, J. M., Wandinger-Ness, A. and Stein, M.-P. (2007). Myotubularin lipid phosphatase binds the hVPS15/hVPS34 lipid kinase complex on endosomes. *Traffic* **8**, 1052-1067.

Cao, C., Backer, J. M., Laporte, J., Bedrick, E. J. and Wandinger-Ness, A. (2008). Sequential actions of myotubularin lipid phosphatases regulate endosomal PI(3)P and growth factor receptor trafficking. *Mol. Biol. Cell* **19**, 3334-3346.

Carlton, J., Bujny, M., Peter, B. J., Oorschot, V. M. J., Rutherford, A., Mellor, H., Klumperman, J., McMahon, H. T. and Cullen, P. J. (2004). Sorting Nexin-1 mediates tubular endosome-to-TGN transport through coincidence sensing of high- curvature membranes and 3-phosphoinositides. *Curr. Biol.* **14**, 1791.

Christoforidis, S., Miaczynska, M., Ashman, K., Wilm, M., Zhao, L., Yip, S.-C., Waterfield, M. D., Backer, J. M. and Zerial, M. (1999). Phosphatidylinositol-3-OH kinases are Rab5 effectors. *Nat. Cell Biol.* **1**, 249.

Cozier, G. E., Carlton, J., McGregor, A. H., Gleeson, P. A., Teasdale, R. D., Mellor, H. and Cullen, P. J. (2002). The phox homology (PX) domain-dependent, 3-phosphoinositide-mediated association of sorting nexin-1 with an early sorting endosomal compartment is required for its ability to regulate epidermal growth factor receptor degradation. *J. Biol. Chem.* **277**, 48730-48736.

Daro, E., van der Sluijs, P., Galli, T. and Mellman, I. (1996). Rab4 and cellubrevin define different early endosome populations on the pathway of Tfn receptor recycling. *Proc. Natl. Acad. Sci. USA* **93**, 9559-9564.

Dove, S. K., McEwen, R. K., Mayes, A., Hughes, D. C., Beggs, J. D. and Michell, R. H. (2002). Vac14 controls PtdIns(3,5)P₂ synthesis and Fab1-dependent protein trafficking to the multivesicular body. *Curr. Biol.* **12**, 885.

Dove, S. K., Dong, K., Kobayashi, T., Williams, F. K. and Michell, R. H. (2009). Phosphatidylinositol 3,5-bisphosphate and Fab1p/PIKfyve underPPIn endo-lysosome function. *Biochem. J.* **419**, 1-13.

Dussault, A. A. and Pouliot, M. (2006). Rapid and simple comparison of messenger RNA levels using real-time PCR. *Biol. Proced. Online* **8**, 1-10.

Fili, N., Calleja, V., Woscholski, R., Parker, P. J. and Larijani, B. (2006). Compartmental signal modulation: endosomal phosphatidylinositol 3-phosphate controls endosome morphology and selective cargo sorting. *Proc. Natl. Acad. Sci. USA* **103**, 15473-15478.

Furutani, M., Tsujita, K., Itoh, T., Ijuin, T. and Takenawa, T. (2006). Application of phosphoinositide-binding domains for the detection and quantification of specific phosphoinositides. *Anal. Biochem.* **355**, 8-18.

Galli, T., Chilcote, T., Mundigl, O., Binz, T., Niemann, H. and De Camilli, P. (1994). Tetanus toxin-mediated cleavage of cellubrevin impairs exocytosis of Tfn receptor-containing vesicles in CHO cells. *J. Cell Biol.* **125**, 1015-1024.

Gary, J. D., Wurmser, A. E., Bonangelino, C. J., Weisman, L. S. and Emr, S. D. (1998). Fab1p is essential for PtdIns(3)P 5-Kinase activity and the maintenance of vacuolar size and membrane homeostasis. *J. Cell Biol.* **143**, 65-79.

Gaullier, J. M., Simonsen, A., D'Arrigo, A., Bremnes, B., Stenmark, H. and Aasland, R. (1998). FYVE fingers bind PtdIns(3)P. *Nature* **394**, 432-433.

Gaullier, J. M., Gillooly, D., Simonsen, A. and Stenmark, H. (1999). Regulation of endocytic membrane traffic by phosphatidylinositol 3-phosphate. *Biochem. Soc. Trans.* **27**, 666-670.

Gillooly, D. J., Morrow, I. C., Lindsay, M., Gould, R., Bryant, N. J., Gaullier, J.-M., Parton, R. G. and Stenmark, H. (2000). Localization of phosphatidylinositol 3-phosphate in yeast and mammalian cells. *EMBO J.* **19**, 4577-4588.

Gillooly, D. J., Raiborg, C. and Stenmark, H. (2003). Phosphatidylinositol 3-phosphate is found in microdomains of early endosomes. *Histochem. Cell Biol.* **120**, 445-453.

Gorvel, J.-P., Chavrier, P., Zerial, M. and Gruenberg, J. (1991). rab5 controls early endosome fusion in vitro. *Cell* **64**, 915.

Gruenberg, J. (2001). The endocytic pathway: a mosaic of domains. *Nat. Rev. Mol. Cell Biol.* **2**, 721-730.

Hao, M. and Maxfield, F. R. (2000). Characterization of rapid membrane internalization and recycling. *J. Biol. Chem.* **275**, 15279-15286.

Hopkins, C. R. and Trowbridge, I. S. (1983). Internalization and processing of Tfn and the Tfn receptor in human carcinoma A431 cells. *J. Cell Biol.* **97**, 508-521.

Hopkins, C. R., Gibson, A., Shipman, M., Strickland, D. K. and Trowbridge, I. S. (1994). In migrating fibroblasts, recycling receptors are concentrated in narrow tubules in the pericentriolar area, and then routed to the plasma membrane of the leading lamella. *J. Cell Biol.* **125**, 1265-1274.

Hunyady, L., Baukal, A. J., Gaborik, Z., Olivares-Reyes, J. A., Bor, M., Szaszak, M., Lodge, R., Catt, K. J. and Balla, T. (2002). Differential PI 3-kinase dependence of early and late phases of recycling of the internalized AT1 angiotensin receptor. *J. Cell Biol.* **157**, 1211-1222.

Ikonomov, O. C., Sbrissa, D. and Shisheva, A. (2001). Mammalian cell morphology and endocytic membrane homeostasis require enzymatically active phosphoinositide 5-kinase PIKfyve. *J. Biol. Chem.* **276**, 26141-26147.

Ikonomov, O. C., Sbrissa, D., Mlak, K., Kanzaki, M., Pessin, J. and Shisheva, A. (2002). functional dissection of lipid and protein kinase signals of PIKfyve reveals the role of PtdIns 3,5-P2 production for endomembrane integrity. *J. Biol. Chem.* **277**, 9206-9211.

Ikonomov, O. C., Sbrissa, D., Foti, M., Carpentier, J.-L. and Shisheva, A. (2003). PIKfyve controls fluid phase endocytosis but not recycling/degradation of endocytosed receptors or sorting of procathepsin d by regulating multivesicular body morphogenesis. *Mol. Biol. Cell* **14**, 4581-4591.

Johnson, E. E., Overmeyer, J. H., Gunning, W. T. and Maltese, W. A. (2006). Gene silencing reveals a specific function of hVps34 phosphatidylinositol 3-kinase in late versus early endosomes. *J. Cell Sci.* **119**, 1219-1232.

Kim, S.-A., Taylor, G. S., Torgersen, K. M. and Dixon, J. E. (2002). Myotubularin and MTMR2, phosphatidylinositol 3-phosphatases mutated in myotubular myopathy and type 4b Charcot-Marie-Tooth disease. *J. Biol. Chem.* **277**, 4526-4531.

Kim, S.-A., Vacratsis, P. O., Firestein, R., Cleary, M. L. and Dixon, J. E. (2003). Regulation of myotubularin-related (MTMR)2 phosphatidylinositol phosphatase by MTMR5, a catalytically inactive phosphatase. *Proc. Natl. Acad. Sci. USA* **100**, 4492-4497.

Laporte, J., Hu, L. J., Kretz, C., Mandel, J.-L., Kioschis, P., Coy, J. F., Klauck, S. M., Poustka, A. and Dahl, N. (1996). A gene mutated in X-linked myotubular myopathy defines a new putative tyrosine phosphatase family conserved in yeast. *Nat. Genet.* **13**, 175-182.

Laporte, J., Liaubet, L., Blondeau, F., Tronchere, H., Mandel, J.-L. and Payrastre, B. (2002). functional redundancy in the myotubularin family. *Biochem. Biophys. Res. Commun.* **291**, 305-312.

Lawe, D. C., Chawla, A., Merithew, E., Dumas, J., Carrington, W., Fogarty, K., Lifshitz, L., Tuft, R., Lambright, D. and Corvera, S. (2002). Sequential roles for phosphatidylinositol 3-phosphate and rab5 in tethering and fusion of early endosomes via their interaction with EEA1. *J. Biol. Chem.* **277**, 8611-8617.

Leonard, D., Hayakawa, A., Lawe, D., Lambright, D., Bellve, K. D., Standley, C., Lifshitz, L. M., Fogarty, K. E. and Corvera, S. (2008). Sorting of EGF and Tfn at the plasma membrane and by cargo-specific signaling to EEA1-enriched endosomes. *J. Cell Sci.* **121**, 3445-3458.

Lin, J. W., Ju, W., Foster, K., Lee, S. H., Ahmadian, G., Wyszynski, M., Wang, Y. T. and Sheng, M. (2000). Distinct molecular mechanisms and divergent endocytotic pathways of AMPA receptor internalization. *Nat. Neurosci.* **3**, 1282-1290.

Lindsay, A. J. and McCaffrey, M. W. (2002). Rab11-FIP2 Functions in Tfn recycling and associates with endosomal membranes via its COOH-terminal domain. *J. Biol. Chem.* **277**, 27193-27199.

Lorenzo, O., Urbe, S. and Clague, M. J. (2005). Analysis of phosphoinositide binding domain properties within the myotubularin-related protein MTMR3. *J. Cell Sci.* **118**, 2005-2012.

Lorenzo, O., Urbe, S. and Clague, M. J. (2006). Systematic analysis of myotubularins: heteromeric interactions, subcellular localisation and endosome related functions. *J. Cell Sci.* **119**, 2953-2959.

Martys, J. L., Wjasow, C., Gangi, D. M., Kielian, M. C., McGraw, T. E. and Backer, J. M. (1996). Wortmannin-sensitive trafficking pathways in Chinese hamster ovary cells. *J. Biol. Chem.* **271**, 10953-10962.

Maxfield, F. R. and McGraw, T. E. (2004). Endocytic recycling. *Nat. Rev. Mol. Cell Biol.* **5**, 121.

McBride, H. M., Rybin, V., Murphy, C., Giner, A., Teasdale, R. and Zerial, M. (1999). Oligomeric complexes link Rab5 effectors with NSF and drive membrane fusion via interactions between EEA1 and syntaxin 13. *Cell* **98**, 377.

McMahon, H. T., Ushkaryov, Y. A., Edelmann, L., Link, E., Binz, T., Niemann, H., Jahn, R. and Sudhof, T. C. (1993). Cellubrevin is a ubiquitous tetanus-toxin substrate homologous to a putative synaptic vesicle fusion protein. *Nature* **364**, 346.

Mesa, R., Magadan, J., Barbieri, A., Lopez, C., Stahl, P. D. and Mayorga, L. S. (2005). Overexpression of Rab22a hampers the transport between endosomes and the Golgi apparatus. *Exp. Cell Res.* **304**, 339-353.

Mochizuki, Y. and Majerus, P. W. (2003). Characterization of myotubularin-related protein 7 and its binding partner, myotubularin-related protein 9. *Proc. Natl. Acad. Sci. USA* **100**, 9768-9773.

Murray, R. Z., Kay, J. G., Sangermani, D. G. and Stow, J. L. (2005). A role for the phagosome in cytokine secretion. *Science* **310**, 1492-1495.

Nandurkar, H. H., Layton, M., Laporte, J., Selan, C., Corcoran, L., Caldwell, K. K., Mochizuki, Y., Majerus, P. W. and Mitchell, C. A. (2003). Identification of myotubularin as the lipid phosphatase catalytic subunit associated with the 3-phosphatase adapter protein, 3-PAP. *Proc. Natl. Acad. Sci. USA* **100**, 8660-8665.

Nichols, B. J., Kenworthy, A. K., Polishchuk, R. S., Lodge, R., Roberts, T. H., Hirschberg, K., Phair, R. D. and Lippincott-Schwartz, J. (2001). Rapid cycling of lipid raft markers between the cell surface and Golgi complex. *J. Cell Biol.* **153**, 529-542.

Nielsen, E., Severin, F., Backer, J. M., Hyman, A. A. and Zerial, M. (1999). Rab5 regulates motility of early endosomes on microtubules. *Nat. Cell Biol.* **1**, 376.

Nielsen, E., Christoforidis, S., Uttenweiler-Joseph, S., Miaczynska, M., Dewitte, F., Wilm, M., Hoflack, B. and Zerial, M. (2000). Rabenosyn-5, a novel Rab5 effector, is complexed with hVPS45 and recruited to endosomes through a FYVE finger domain. *J. Cell Biol.* **151**, 601-612.

Odorizzi, G., Babst, M. and Emr, S. D. (1998). Fab1p PtdIns(3)P 5-kinase function essential for protein sorting in the multivesicular body. *Cell* **95**, 847-858.

Odorizzi, G., Babst, M. and Emr, S. D. (2000). Phosphoinositide signaling and the regulation of membrane trafficking in yeast. *Trends Biochem. Sci.* **25**, 229-235.

Osborne, S. L., Wen, P. J., Boucheron, C., Nguyen, H. N., Hayakawa, M., Kaizawa, H., Parker, P. J., Vitale, N. and Meunier, F. A. (2008). PIKfyve negatively regulates exocytosis in neurosecretory cells. *J. Biol. Chem.* **283**, 2804-2813.

Panopoulou, E., Gillooly, D. J., Wrana, J. L., Zerial, M., Stenmark, H., Murphy, C. and Fotsis, T. (2002). Early endosomal regulation of Smad-dependent signaling in endothelial Cells. *J. Biol. Chem.* **277**, 18046-18052.

Park, M., Penick, E. C., Edwards, J. G., Kauer, J. A. and Ehlers, M. D. (2004). Recycling endosomes supply AMPA receptors for LTP. *Science* **305**, 1972-1975.

Petiot, A., Faure, J., Stenmark, H. and Gruenberg, J. (2003). PI3P signaling regulates receptor sorting but not transport in the endosomal pathway. *J. Cell Biol.* **162**, 971-979.

Plant, P. J., Correa, J., Goldenberg, N., Bain, J. and Batt, J. (2009). The inositol phosphatase MTMR4 is a novel target of the ubiquitin ligase Nedd4. *Biochem. J.* **419**, 57-63.

Polgar, J., Chung, S.-H. and Reed, G. L. (2002). Vesicle-associated membrane protein 3 (VAMP-3) and VAMP-8 are present in human platelets and are required for granule secretion. *Blood* **100**, 1081-1083.

Ren, M., Xu, G., Zeng, J., De Lemos-Chiarandini, C., Adesnik, M. and Sabatini, D. D. (1998). Hydrolysis of GTP on rab11 is required for the direct delivery of Tfn from the pericentriolar recycling compartment to the cell surface but not from sorting endosomes. *Proc. Natl. Acad. Sci. USA* **95**, 6187-6192.

Robinson, F. L. and Dixon, J. E. (2005). The phosphoinositide-3-phosphatase MTMR2 associates with MTMR13, a membrane-associated pseudophosphatase also mutated in type 4B Charcot-Marie-Tooth disease. *J. Biol. Chem.* **280**, 31699-31707.

Robinson, F. L. and Dixon, J. E. (2006). Myotubularin phosphatases: policing 3-phosphoinositides. *Trends Cell Biol.* **16**, 403.

Rojas, R., Kametaka, S., Haft, C. R. and Bonifacino, J. S. (2007). Interchangeable but essential functions of SNX1 and SNX2 in the association of retromer with endosomes and the trafficking of mannose 6-phosphate receptors. *Mol. Cell. Biol.* **27**, 1112-1124.

Rutherford, A. C., Traer, C., Wassmer, T., Pattni, K., Bujny, M. V., Carlton, J. G., Stenmark, H. and Cullen, P. J. (2006). The mammalian phosphatidylinositol 3-phosphate 5-kinase (PIKfyve) regulates endosome-to-TGN retrograde transport. *J. Cell Sci.* **119**, 3944-3957.

Saraste, J. and Goud, B. (2007). Functional symmetry of endomembranes. *Mol. Biol. Cell* **18**, 1430-1436.

Schaletzky, J., Dove, S. K., Short, B., Lorenzo, O., Clague, M. J. and Barr, F. A. (2003). Phosphatidylinositol-5-phosphate activation and conserved substrate specificity of the myotubularin phosphatidylinositol 3-phosphatases. *Curr. Biol.* **13**, 504-509.

Senderek, J., Bergmann, C., Weber, S., Ketelsen, U.-P., Schorle, H., Rudnik-Schoneborn, S., Buttner, R., Buchheim, E. and Zerres, K. (2003). Mutation of the SBF2 gene, encoding a novel member of the myotubularin family, in Charcot-Marie-Tooth neuropathy type 4B2/11p15. *Hum. Mol. Genet.* **12**, 349-356.

Sheff, D. R., Daro, E. A., Hull, M. and Mellman, I. (1999). The receptor recycling pathway contains two distinct populations of early endosomes with different sorting functions. *J. Cell Biol.* **145**, 123-139.

Sheff, D., Pelletier, L., O'Connell, C. B., Warren, G. and Mellman, I. (2002). Tfn receptor recycling in the absence of perinuclear recycling endosomes. *J. Cell Biol.* **156**, 797-804.

Shin, H.-W., Hayashi, M., Christoforidis, S., Lacas-Gervais, S., Hoepfner, S., Wenk, M. R., Modregger, J., Uttenweiler-Joseph, S., Wilm, M., Nystuen, A. et al. (2005). An enzymatic cascade of Rab5 effectors regulates phosphoinositide turnover in the endocytic pathway. *J. Cell Biol.* **170**, 607-618.

Shpetner, H., Joly, M., Hartley, D. and Corvera, S. (1996). Potential sites of PI-3 kinase function in the endocytic pathway revealed by the PI-3 kinase inhibitor, wortmannin. *J. Cell Biol.* **132**, 595-605.

Simpson, J. C., Griffiths, G., Wessling-Resnick, M., Fransen, J. A. M., Bennett, H. and Jones, A. T. (2004). A role for the small GTPase Rab21 in the early endocytic pathway. *J. Cell Sci.* **117**, 6297-6311.

Smythe, E. (2002). Direct interactions between rab GTPases and cargo. *Mol. Cell* **9**, 205-206.

Sonnichsen, B., De Renzis, S., Nielsen, E., Rietdorf, J. and Zerial, M. (2000). Distinct membrane domains on endosomes in the recycling pathway visualized by multicolor imaging of Rab4, Rab5, and Rab11. *J. Cell Biol.* **149**, 901-914.

Spiro, D., Boll, W., Kirchhausen, T. and Wessling-Resnick, M. (1996). Wortmannin alters the Tfn receptor endocytic pathway in vivo and in vitro. *Mol. Biol. Cell* **7**, 355-367.

Szekeres, P. G., Koenig, J. A. and Edwardson, J. M. (1998). Involvement of receptor cycling and receptor reserve in resensitization of muscarinic responses in SH-SY5Y human neuroblastoma cells. *J. Neurochem.* **70**, 1694-1703.

Taylor, G. S. and Dixon, J. E. (2004). Assaying phosphoinositide phosphatases. *Methods Mol. Biol.* **284**, 217-227.

Taylor, G. S., Maehama, T. and Dixon, J. E. (2000). Inaugural article: Myotubularin, a protein tyrosine phosphatase mutated in myotubular myopathy, dephosphorylates the lipid second messenger, phosphatidylinositol 3-phosphate. *Proc. Natl. Acad. Sci. USA* **97**, 8910-8915.

Tronchere, H., Laporte, J., Pendaries, C., Chaussade, C., Liaubet, L., Pirola, L., Mandel, J.-L. and Payrastre, B. (2004). Production of phosphatidylinositol 5-phosphate by the phosphoinositide 3-phosphatase myotubularin in mammalian cells. *J. Biol. Chem.* **279**, 7304-7312.

Tsujita, K., Itoh, T., Ijuin, T., Yamamoto, A., Shisheva, A., Laporte, J. and Takenawa, T. (2004). Myotubularin regulates the function of the late endosome through the GRAM domain-phosphatidylinositol 3,5-bisphosphate interaction. *J. Biol. Chem.* **279**, 13817-13824.

Ullrich, O., Reinsch, S., Urbe, S., Zerial, M. and Parton, R. G. (1996). Rab11 regulates recycling through the pericentriolar recycling endosome. *J. Cell Biol.* **135**, 913-924.

van Dam, E. M. and Stoorvogel, W. (2002). Dynamin-dependent Tfn receptor recycling by endosome-derived clathrin-coated vesicles. *Mol. Biol. Cell* **13**, 169-182.

van Dam, E. M., ten Broeke, T., Jansen, K., Spijkers, P. and Stoorvogel, W. (2002). Endocytosed Tfn receptors recycle via distinct dynamin and phosphatidylinositol 3-kinase-dependent pathways. *J. Biol. Chem.* **277**, 48876-48883.

Walker, D. M., Urbe, S., Dove, S. K., Tenza, D., Raposo, G. and Clague, M. J. (2001). Characterization of MTMR3, an inositol lipid 3-phosphatase with novel substrate specificity. *Curr. Biol.* **11**, 1600-1605.

Wilcke, M., Johannes, L., Galli, T., Mayau, V., Goud, B. and Salamero, J. (2000). Rab11 Regulates the compartmentalization of early endosomes required for efficient transport from early endosomes to the trans-Golgi network. *J. Cell Biol.* **151**, 1207-1220.

Yu, J., Pan, L., Qin, X., Chen, H., Xu, Y., Chen, Y. and Tang, H. (2010). MTMR4 attenuates transforming growth factor beta (TGFbeta) signaling by dephosphorylating R-Smads in endosomes. *J. Biol. Chem.* **285**, 8454-8462.

Zhang, X.-M., Ellis, S., Sriratana, A., Mitchell, C. A. and Rowe, T. (2004). Sec15 is an effector for the rab11 GTPase in mammalian cells. *J. Biol. Chem.* **279**, 43027-43034.

Zhao, Y. and Keen, J. H. (2008). Gyrating clathrin: highly dynamic clathrin structures involved in rapid receptor recycling. *Traffic* **9**, 2253-2264.

Zhao, R., Qi, Y., Chen, J. and Zhao, Z. J. (2001). FYVE-DSP2, a fyve domain-containing dual specificity protein phosphatase that dephosphorylates phosphotidylinositol 3-phosphate. *Exp. Cell Res.* **265**, 329-338.